Abstract: We propose the design of a novel γ-shaped fiber laser resonator and apply it to build a long-cavity normal-dispersion mode-locked Er-fiber laser which features enhanced functionalities for management and optimization of pulsed lasing regimes. We report the generation of sub-nanosecond pulses with the energy of ~ 0.5 μJ at a kilohertz-scale repetition rate in an all-fiber system based on the new laser design. A combination of special design solutions in the laser, such as polarization instability compensation in the ultra-long arm of the resonator, intra-cavity spectral selection of radiation with a broadband fiber Bragg grating, and polarization selection by means of a tilted refractive index grating, ensures low amplified spontaneous emission (ASE) noise and high stability of the laser system output parameters.

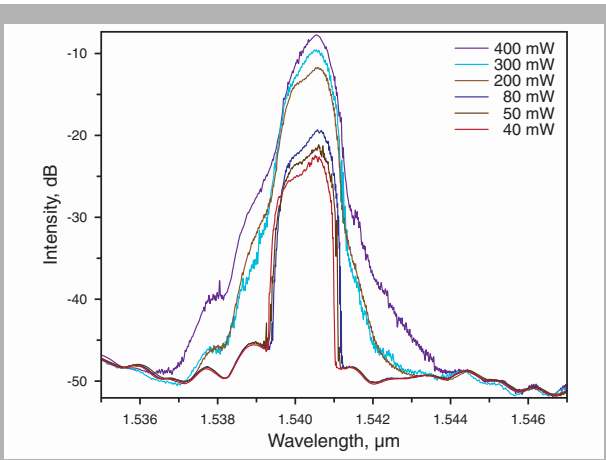

Laser radiation optical spectra acquired at different pumping power levels

Gamma-shaped long-cavity normal-dispersion mode-locked Er-fiber laser for sub-nanosecond high-energy pulsed generation

B.N. Nyushkov, [1,2,*] *A.V. Ivanenko,* [2,3] *S.M. Kobtsev,* [2] *S.K. Turitsyn,* [3] *C. Mou,* [3] *L. Zhang,* [3] *V.I. Denisov,* [1] *and V.S. Pivtsov* [1]

[1] Institute of Laser Physics of SB RAS, 13/3, Ac. Lavrentyev Prosp., Novosibirsk 630090, Russia
[2] Department of Laser Physics and Innovation Technologies, Novosibirsk State University, 2, Pirogov Str., Novosibirsk 630090, Russia
[3] Photonics Research Group, School of Engineering and Applied Science, Aston University, Birmingham B4 7ET, UK

Received: 29 July 2011, Revised: 30 July 2011, Accepted: 2 August 2011
Published online: 2 November 2011

Key words: mode-locked fiber laser; gamma cavity; normal dispersion; tilted fiber grating; sub-nanosecond pulses; low repetition rate; high pulse energy; ASE suppression; double-pass fiber amplifier

1. Introduction

The development of long-cavity (hundreds of meters to several kilometers) passively mode-locked fiber lasers for the generation of high-energy light pulses with relatively low (sub-megahertz) repetition rates has emerged as a new rapidly advancing area of laser physics. The first demonstration of high pulse energy laser of this type [1] was followed by a number of publications from many research groups on long-cavity Ytterbium and Erbium lasers featuring a variety of configurations with rather different mode-locked operations [2–18]. The substantial interest to this new approach is stimulated both by non-trivial underlying physics and by the potential of high pulse energy laser sources with unique parameters for a range of applications in industry, bio-medicine, metrology, and telecommunications.

At present, the highest pulse energy achieved in long-cavity fiber lasers was demonstrated in systems, exploit-

* Corresponding author: e-mail: nyushkov@laser.nsc.ru

ing the effect of nonlinear polarization evolution (NPE) for self-mode-locking operation. In lasers of this type, the pulse energy of several microjoules was demonstrated [1, 8, 11] without using any traditional methods such as Q-switching or cavity dumping techniques. In lasers using saturable absorbers, e.g. conventional semiconductor saturable absorber mirrors (SESAM) [3–5, 17] or substances based on single-wall carbon nanotubes (SWNT) [6, 12], the maximal pulse energy does not exceed several dozens of nanojoules. This can be explained both by limited modulation capabilities of these absorbers (characterization of SWNT-based absorbers was performed in [19]) and by the peculiarities of the dynamics of pulsed generation in high-energy long-cavity fiber lasers. Long-cavity pulsed fiber lasers based on the non-linear optical loop mirrors (NOLM) also feature relatively small pulse energies [2, 18].

Studied long-cavity pulsed fiber lasers differ not only by the mechanisms of mode-locking, but also by their resonator layouts. Most of the considered lasers are based on the conventional ring configuration – the simplest to set up and requiring no reflectors. Lasers based on NOLM, respectively, have figure-eight cavities. Lasers using SESAMs for mode-locking, typically utilize linear Fabry-Perot [5, 7] or ring-linear cavity layouts with a short linear arm [3, 4, 17]. Of a particular interest is the linear-ring cavity design [10, 11], in which a longer section of the optical fiber is in the linear arm ended by a Faraday mirror. This solution ensures suppression or elimination of polarization-induced fluctuations, thus improving the stability of laser output parameters when low cost non-polarization-maintaining fibers are used. Besides, the linear-ring configuration can provide almost a factor-of-two advantage in the output pulse energy using the same physical length of the resonator due to repetition rate being twice as low as that in a traditional ring laser of the same length. Another original solution was demonstrated in a long-cavity laser [12] fabricated with the use of polarization-maintaining fibers. The pulse repetition rate in such "θ-configuration" resonator is twice as low as in a conventional ring laser of the same fiber length.

It is well known, that pulse generation regimes in mode-locked fiber lasers are determined by the intra-cavity balance between the effects of dispersion and nonlinearity, and the processes of energy attenuation and amplification. In case when the dissipation plays a decisive role in the pulse dynamics, e.g. in fiber lasers with normal intra-cavity dispersion, it is possible to generate the so-called dissipative optical solitons [20–24]. The combination of dissipative soliton lasing and laser cavity lengthening makes possible a considerable increase in the pulse energy with a corresponding reduction in the repetition rate, at the same time preserving stable mode-locking operation with one pulse per cavity period. On the other hand, the uncompensated net normal dispersion in long-cavity resonators usually leads to the giant chirp [6] and, consequently, to a relatively long duration of generated pulses. Moreover, long-cavity normal-dispersion fiber

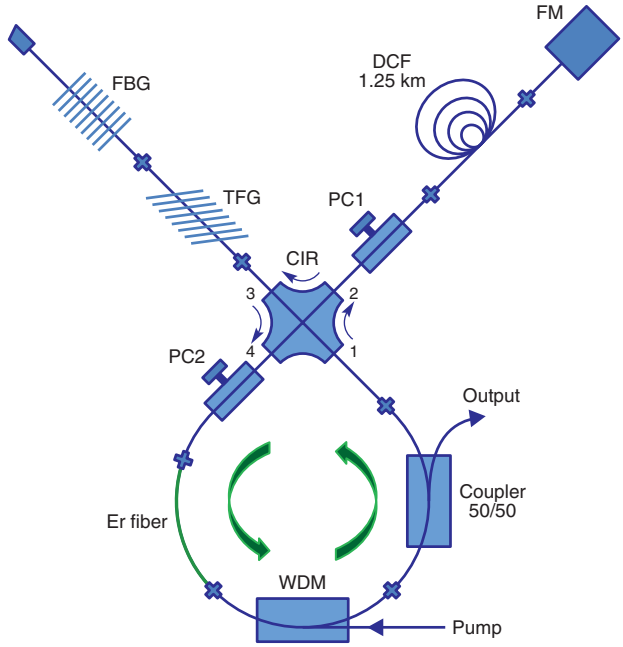

Figure 1 (online color at www.lphys.org) Laser cavity diagram. FBG – fiber Bragg grating, TFG – tilted fiber grating, CIR – circulator, PC – polarization controller, DCF – dispersion compensating fiber, FM – Faraday mirror, and WDM – wavelength-division multiplexer

lasers mode-locked *via* NPE may tend to a noise-like regime generating double-scale optical lumps [25] with a smooth bell-shaped envelope and stochastic ultra-short pulsed filling, unless a careful adjustment of the laser system parameters is implemented. In all cases the observed duration either of single pulses or double-scale lumps in long-cavity pulsed lasers with normal dispersion varies from few to dozens of nanoseconds. Recently proposed and theoretically studied method of extra-cavity dispersive compression of output pulses of such lasers opens a prospect of producing pulses with sub-nanosecond duration without significant reduction in their energy [26].

In long-cavity mode-locked fiber lasers with anomalous dispersion [2, 7, 9, 12] it is possible to generate substantially shorter, typically, picosecond scale pulses. However, their energy is low, typically not exceeding 20 nJ. Further energy growth is limited by nonlinear effects leading to pulse decomposition and transition to multi-pulse generation mode. The related limitations of pulse shaping in anomalous-dispersion mode-locked fiber lasers are explained in [27] and [35]. Nevertheless, with a proper resonator management, as demonstrated recently, it is feasible to generate high-energy pulses even in long-cavity fiber lasers with anomalous dispersion. However, these high-energy pulses possess properties similar to those of dissipative solitons and have a relatively long (nanosecond) duration as well [14, 15].

The development of novel types of long-cavity mode-locked fiber lasers for the low-repetition-rate generation of wave-breaking-free high-energy pulses with sub-nanosecond duration presents significant challenge with great potential for a range of applications.

The main goal of this work is the development of a long-cavity normal-dispersion mode-locked Er-fiber laser with a special cavity design which features enhanced built-in functionalities for management and optimization of pulsed lasing regimes. This laser has to operate as a master oscillator in an all-fiber laser system (being also studied in this work) capable of the stable generation of sub-nanosecond high-energy pulses at a kilohertz-scale repetition rate along with the efficient suppression of amplified spontaneous emission (ASE). Laser systems with such parameters are required in a range of applied problems, in particular, for the generation of high-energy spectral super-continua [29] and for implementation of cutting-edge methods of absorption spectroscopy [30].

2. Experimental setup

The developed laser has an all-fiber linear-ring resonator that is schematically presented in Fig. 1. One of the key novel points making the difference from our previous designs [10, 11] is that we use an additional linear arm in the resonant cavity. The function of this arm is to sustain mode-locking and to control the spectrum of laser radiation. The proposed here cavity design is based on the use a four-port fiber-optics circulator (CIR) that leads to an original "γ-configuration" of the resonator. It offers additional possibilities for optimization of lasing dynamics and control over the radiation parameters in long-cavity normal-dispersion mode-locked fiber lasers. Another important feature of the proposed laser cavity design is a combination of photo-induced in-fiber refractive index gratings: a traditional fiber Bragg grating (FBG) [31] and a polarizing 45°-tilted fiber grating (TFG) [32, 33]. These elements are used for realization of self-mode-locking and control of the radiation parameters. Such a combination of fiber grating elements has been used for the first time in long-cavity high-energy pulsed lasers.

The functional elements of the laser are distributed along various segments of the resonator in an optimal way as follows. The ring part of the resonator comprises only of the active erbium-doped fiber with a pump multiplexor and an output coupler placed before the circulator. Such positioning allows us to achieve the highest possible output power and to suppress non-linear effects in the longest arm of the resonant cavity. The long arm formed by a reel of a single-mode fiber with normal dispersion is ended by a Faraday mirror. This ensures the elimination, or significant suppression, of polarization-induced fluctuations, which could significantly undermine the stability of mode-locking upon the use of non-polarization-maintaining fibers. The additional short linear arm contains a combination of the above mentioned TFG and FBG spaced as closely as possible. TFG serves a dual purpose: it works as a polarization discriminator for triggering self-mode-locking through the effect of non-linear evolution of polarization state along the fiber [27, 33] as well as prevents the competition of polarization modes typical for fiber lasers with FBGs [34]. FBG acts as a spectral filter allowing for optimization of the generation dynamics, reducing the pulse duration, and improving the stability of the mode-locked operation. Especially, it stabilizes the lasing wavelength and prevents dual-wavelength switchable operation [35]. The technique of pulse shaping by intracavity spectral filtering applicable to mode-locked fiber lasers with normal dispersion (see, e.g. [28, 36] and references therein) has not yet been fully explored with regard to the long-cavity lasers. The only notable attempt to use an intracavity spectral filter in a long-cavity high-energy mode-locked fiber laser for stabilization of the lasing wavelength has been just recently reported in [17]. In the present work we additionally achieve ASE suppression caused by placing a FBG-based bandpass filter into the laser scheme.

The parameters of the fiber-optics elements used in the laser are as follows: Er-fiber – a 1.8-m-long highly-doped fiber with the erbium ion concentration of $\sim 2.1\times10^{19}$ cm^{-3} (Liekki Er30-4/125); DCF – a 1.25-km-long telecom dispersion-compensating fiber with an overall chromatic dispersion of ~ 217 ps^2 and optical losses of ~ 1.3 dB (Sumitomo N-DCFM-C-10-FA); FBG – an UV inscribed fiber Bragg grating with a peak reflectivity of $\sim 95.55\%$, the peak wavelength of ~ 1540.4 nm, and the bandwidth of ~ 2.61 nm; TFG – an UV inscribed tilted fiber grating with a blaze angle of $\sim 45°$, similar to the gratings reported in [32, 33]; CIR – a four-port polarization-insensitive circulator (Opneti CIR-4-A-1550); PC1 and PC2 – in-line polarization controllers; WDM – a 980/1550-nm wavelength division multiplexor; Pump – a 980-nm fiber-coupled pump source with the maximal output power of 400 mW; and Coupler – fused fiber coupler with the 50/50 coupling ratio.

Anomalous-dispersion fiber pigtails of the fiber-optics elements have been cut to minimal possible lengths of 15 – 25 cm. Their contribution into the net intra-cavity dispersion in the vicinity of the generation wavelength is negligible and does not exceed –0.07 ps^2. The amount of the dispersion introduced by the Erbium fiber is also insignificant and makes approximately –0.15 ps^2. Thus, the total intra-cavity dispersion $\sum \beta_2$ with the double-pass connection of DCF taken into account exceeds +433 ps^2.

Specific parameters of certain elements (for example, the FBG bandwidth and the coupling ratio of the output coupler) have been chosen empirically basing on preliminary laser examinations for the following criteria: high reliability of mode-locked lasing, the shortest duration and the highest energy of generated pulses, as well as high stability of the laser output parameters.

The laser output parameters were measured by means of an optical spectrum analyzer having a resolution down to 0.02 nm and a high-frequency oscilloscope equipped

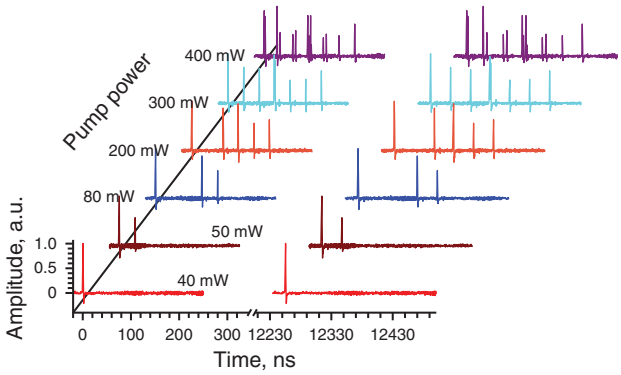

Figure 2 (online color at www.lphys.org) Series of oscillograms acquired from the laser output to illustrate evolution of the laser operation mode (from multi- to single-pulse lasing) with the change of the pump power. The cavity round trip time is ~ 12250 ns

with an ultra-fast photo-diode providing a temporal resolution within 400 ps. In addition, a broadband RF spectrum analyzer was used along with the same ultra-fast photo-diode in order to study intermode beats.

3. Results and discussion

Depending on the parameters of the polarization controllers and the pre-set pumping power launched into the laser, both multi-pulse and single-pulse mode-locked operation can be triggered. The settings also affect the form and the duration of the output pulses. Below we present the results of a study of the two most favorable operation modes leading to stable pulse generation at the fundamental repetition frequency. In the first mode of operation, the shortest pulse duration (~ 1.0 ns) is achieved, with an easily triggered start and high stability. The second operation mode leads to the highest pulse energy. However, it is less stable and with longer pulse duration. The generation dynamics in these two modes exhibits substantial differences. In the first mode, the generation spectrum is considerably narrower than the transmission bandwidth of the intra-cavity FBG-based spectral filter. The effect of this "soft" spectral filtration is in reduction of the ASE level as well as in improvement of the self-mode-locking reliability and stability of the output parameters. In the second mode that is observed at higher pump powers, the generation spectrum becomes noticeably wider than the transmission bandwidth of the intra-cavity filter, i.e. so-called "strong" filtration takes place. The generation dynamics of mode-locked fiber lasers with normal dispersion and "strong" spectral filtering has been theoretically studied in [37]. Such filtering makes it possible to restrain pulse elongation when the pulse energy is increased. Theoretically, this type of lasing dynamics has also been studied for particular laser configurations in [38, 39].

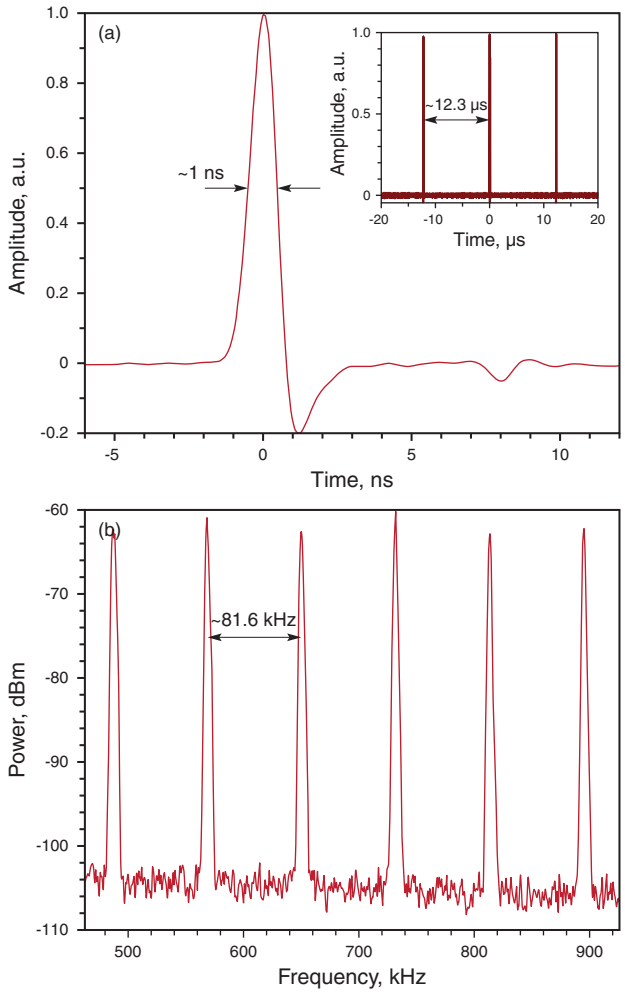

Figure 3 (online color at www.lphys.org) (a) – oscillograms of the laser output during the single-pulse mode-locked operation (mode No. 1): the red line – high resolution trace of a single pulse; the brown line (inset) – trace of the regular pulse train and (b) – intermode beats spectrum acquired during the single-pulse mode-locked operation (mode No. 1)

3.1. Mode No. 1

In general, a hysteresis dependence of the operation mode parameters on the pump power is typical for the considered laser system. When a certain level of pumping power is reached (much higher than the lasing threshold), multi-pulse partially mode-locked operation is self-triggered. In this lasing regime quasi-regular trains of nanosecond pulses are generated. Furthermore, at pump powers exceeding 200 – 250 mW, such trains contain noise-like pulses with an irregular shape of the envelope and stochastic structure. Gradual reduction of the pumping power leads to a corresponding decrease of the number of pulses in the train down to the single-pulse lasing regime (with only one pulse circulating in the cavity). The series of os-

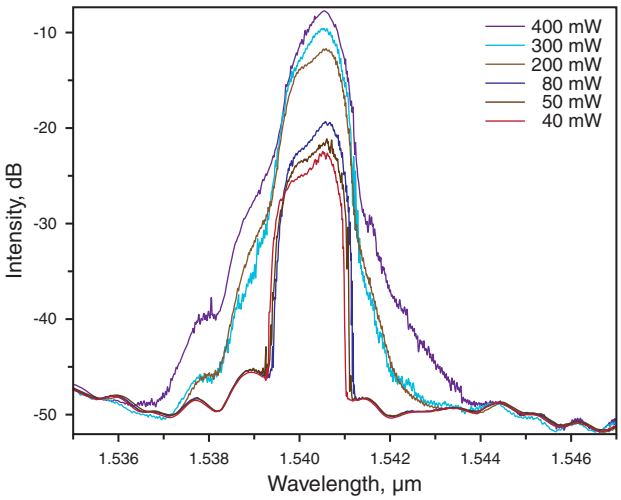

Figure 4 (online color at www.lphys.org) Laser radiation optical spectra acquired at different pumping power levels

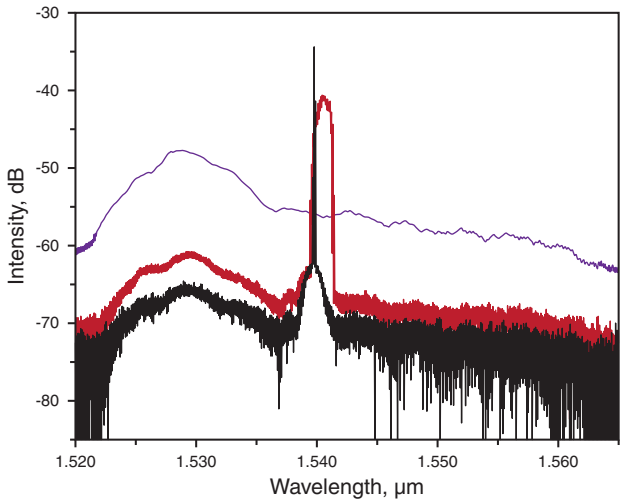

Figure 5 (online color at www.lphys.org) Optical spectra of the laser radiation: the red line corresponds to the single-pulse mode-locked output (operation mode No. 1); the black line – to the continuous-wave (CW) operation mode; the lilac line – to the ASE-source mode (FBG disconnected)

cillograms in Fig. 2 illustrates such transition from multi-pulse lasing to the single-pulse operation mode as the launched pump power is reduced from 400 to 40 mW. Duration of the resulting pulse is ~ 1.0 ns, as appears from the high-resolution oscillogram in Fig. 3a. The pulse train emitted from the laser operating in this mode is regular, with the pulse interval equal to the cavity round-trip time (~ 12.25 μs) as shown in the insert of Fig. 3a. The pulse repetition rate corresponds to the fundamental repetition frequency of ~ 81.6 kHz that is determined by the cavity round trip time. Examination of intermode beats spectra using a broadband radio frequency (RF) spectrum analyzer has shown high spectral purity and good frequency stability. Even for high-order beats (at frequencies ~ 1 MHz) the signal/noise ratio is higher than 45 dB (see the RF-spectrum in Fig. 3b). The measured intermode frequency is equal to the pulse repetition rate. Thus, the acquired data indicate strong mode-locking in the laser set to operate in the described single-pulse regime. This operation mode (hereinafter "operation mode No. 1") is very stable with respect to any environmental perturbations and fluctuations of the pump power; it can be continuously maintained throughout a day.

The character of the evolution of the laser optical spectrum (Fig. 4) during the transition from the multi-pulse lasing to the single-pulse operation mode No. 1 is in partial agreement with the spectrum variation demonstrated in [40] that occurs when the pump power is changing. However, the mechanism of emergence of the noise-like pulses at high pump powers in our laser is most probably different than the "peak power clamping effect" pointed out in [40]. In our case pulse trains occur at a repetition frequency different from the fundamental one and are not always uniformly distributed over the cavity perimeter. The major factor leading to the occurrence of such irregular pulses is likely to be related to wave breaking that takes place when the peak power exceeds a certain threshold. This might be also closely linked to the wave collapse mechanisms proposed and studied in [41,42]. Another physical mechanism giving rise to wave breaking in ultra-long lasers may be perturbations caused by a strong ASE.

Despite the moderate average output power (~ 1.5 mW) of the laser in the operation mode No. 1, the very low pulse repetition rate allows presumably for accumulation of sufficiently high energy in the generated pulses. However, a realistic estimate of the pulse energy requires consideration of ASE contribution to the laser output.

Indeed, in long-cavity mode-locked fiber lasers, a considerable fraction of the pump energy may be converted into ASE, because of a significant cavity round-trip time and long pulse-to-pulse intervals. For example, in the long-cavity erbium laser [12], the energy fraction of ASE was as high as 10 to 50% depending on the pulse repetition rate. In our case, the addition of an FBG-based spectral filter has resulted in a substantial reduction of ASE in the laser, which is most noticeable at high pumping powers. Energy contribution of ASE into the output radiation has been estimated by integration of the power spectral density in the single-pulse mode-locked output, in the continuous wave mode, and in the ASE-source mode (with the FBG being disconnected), all at the same level of the pumping power.

Output spectra in these modes of operation are presented in Fig. 5 (the average radiation power at the input of the spectrum analyzer is the same in all cases). Thus, in the studied single-pulse operation mode No. 1, the energy proportion of ASE in the output radiation does not exceed,

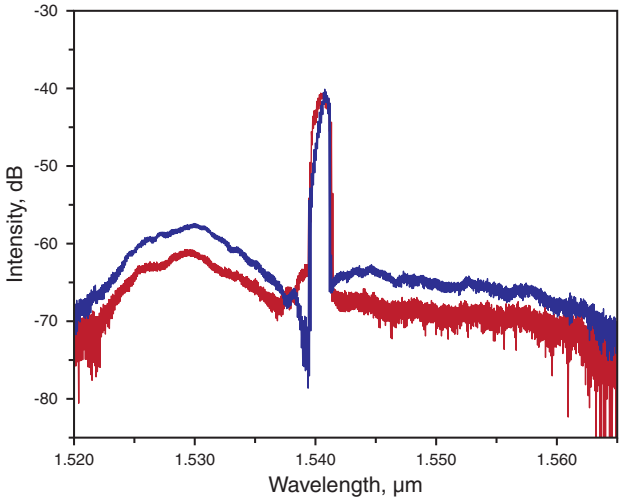

Figure 6 (online color at www.lphys.org) Optical spectra of the laser radiation during the single-pulse operation mode No. 1: the red line corresponds to the spectrum normally acquired from the output coupler; the blue line – to the spectrum acquired from the FBG

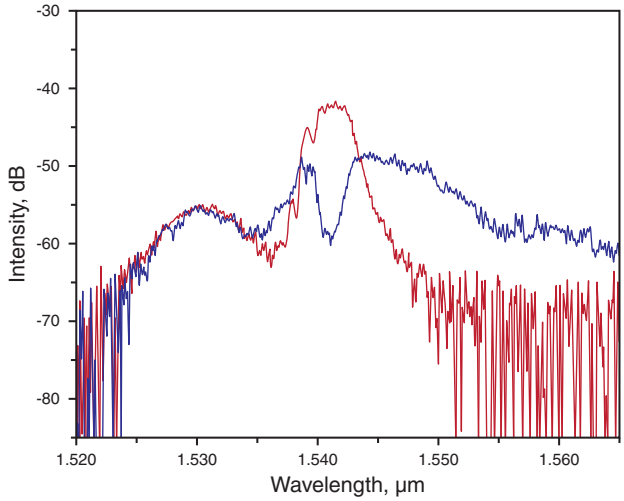

Figure 8 (online color at www.lphys.org) Optical spectra of the laser radiation during the single-pulse operation mode No. 2: the red line corresponds to the spectrum normally acquired from the output coupler and the blue line – to the spectrum acquired from the FBG

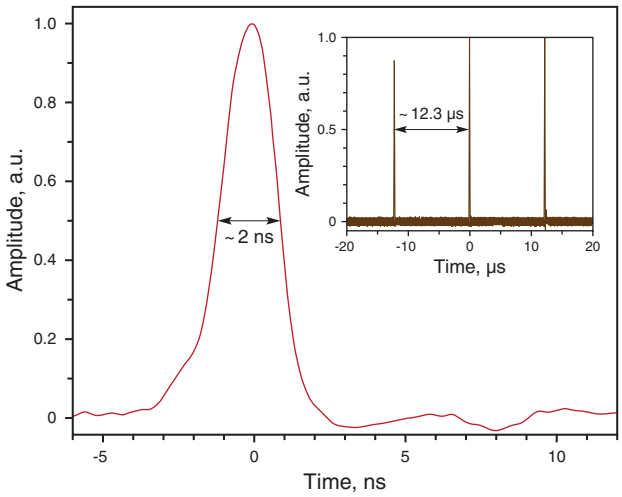

Figure 7 (online color at www.lphys.org) Oscillograms of the laser output during the single-pulse operation mode No. 2: the red line – high resolution trace of a single pulse and the brown line (inset) – trace of the regular pulse train

according to our estimate, 5%. A realistic estimate then of the output pulse energy taking into account the ASE factor yields a value of ~ 17.5 nJ.

The effect of intra-cavity spectral filtering on the ASE suppression is noticeable even at low pump levels. As seen in Fig. 6, a comparison of the laser radiation spectrum normally acquired from the output coupler and the spectrum acquired from the FBG confirms this conclusion in the case of single-pulse operation mode No. 1. One can see that the spectral power density of ASE components registered at the extracavity pigtail of the FBG is higher than that at the exit port of the output coupler.

3.2. Mode No. 2

Single-pulse mode-locked operation with the "strong" intracavity spectral filtering is initiated at the maximal pumping power through re-tuning of the both polarization controllers. In this mode, pulses with duration of approximately 2 ns are generated (see the oscillogram in Fig. 7). Their optical spectrum that is wider than the transmission band of the intra-cavity filter. A comparison of the laser radiation spectrum normally acquired from the output coupler and the spectrum acquired from the FBG stresses the effect of spectral profiling (see Fig. 8). The FBG-based bandpass filter not only cuts away the ASE components in the radiation spectrum, but also narrows the pulse spectrum itself, which gets broadened again due to non-linear effects during a subsequent resonator trip.

The average output power in the described operation mode (hereinafter "operation mode No. 2") reaches approximately 8 mW, with the ASE contribution not exceeding 15%. Correspondingly, the pulse energy may reach ~ 83.3 nJ. This mode is less stable than the first single-pulse operation mode and the output pulses are subject to decomposition under strong environmental perturbations or fluctuations of the pumping power. Most likely, wave breaking of these pulses having a sufficiently high peak

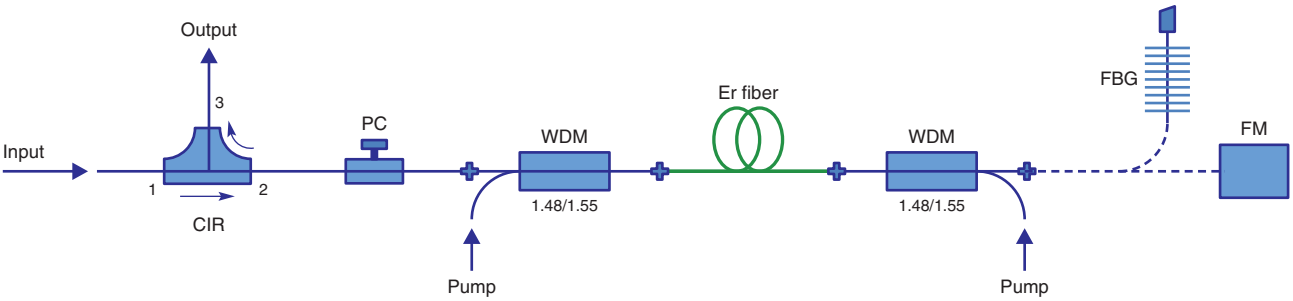

Figure 9 (online color at www.lphys.org) Diagram of the double-pass EDFA: CIR – circulator, PC – polarization controller, WDM – wavelength-division multiplexer, FBG – fiber Bragg grating, and FM – Faraday mirror

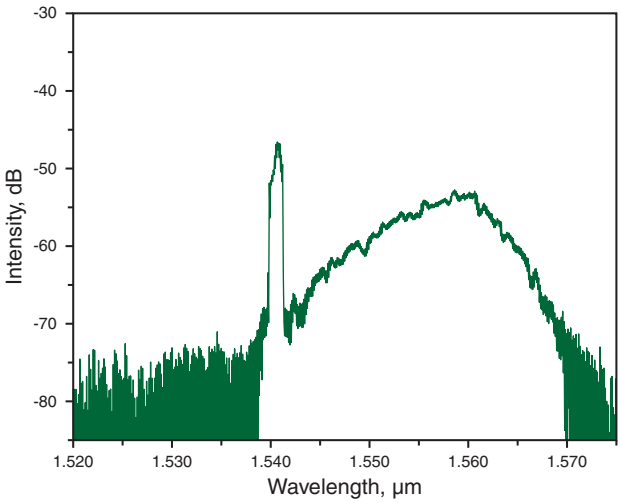

Figure 10 (online color at www.lphys.org) Optical spectrum of the laser radiation upon amplification in the double-pass EDFA with a Faraday mirror

power is catalyzed by a high level of ASE noise. Therefore the operation mode No. 2 does not last a long time. In a few minutes (at the latest) the laser turns to a multi-pulse partially mode-locked lasing regime. The laser output has finally an intensity temporal distribution similar to the oscilloscope traces on top of Fig. 2 (the traces acquired at high pump power levels).

Basing on the above results, we have chosen the first single-pulse operation mode, as being the most stable, low-noise, and short-pulsed, to work on the "master-oscillator-power-amplifier" system described in the following section.

3.3. Amplification and compression

For further augmentation of the pulse energy, an erbium-doped fiber amplifier (EDFA) with a double-pass configuration was used as shown in Fig. 9. The double pass of laser radiation through the EDFA was arranged by means of a conventional three-port circulator and a Faraday mirror (which is finally replaced by a FBG). The circulator serves both as a unidirectional input and a unidirectional output providing, thus, due optical isolation of the amplifying stage. In order to achieve high gain and to minimize non-linear effects, we make use of a heavily doped erbium fiber (Liekki Er80-8/125) which features a large effective mode area and a very high erbium concentration ($\sim 4.7\times10^{19}$ cm^{-3}). The length of this fiber is ~ 1.5 m. It is core-pumped at both ends by means of 1480-nm fiber-coupled laser diodes delivering ~ 350 mW each one.

When a Faraday mirror was used, the average radiation power measured at the amplifier output reached ~ 116 mW. However, the spectrum diagram of the amplified laser radiation (Fig. 10) makes it obvious that the most of this power was distributed into ASE components (up to 71%). Taking this proportion into account, it was estimated that the real energy in the output pulses after amplification did not exceed ~ 412 nJ. It is interesting to note that the above-mentioned spectrum contains practically no short-wavelength ASE components. This may be explained by a sharply limited (from the short-wavelength side) transmission bandwidth of the multiplexors (WDM) used the EDFA for injection of the pump radiation.

In order to reduce the total level of ASE, the Faraday mirror was replaced by an FBG (similar to the grating used in the laser itself). Performing the function of a band-pass filter, the FBG ensures efficient suppression of long-wavelength ASE components, as evidenced by the radiation spectrum acquired from the amplifier output (Fig. 11). When the FBG is used, the average output power reaches ~ 40 mW, the energy proportion of ASE amounts to less than 3%, and the improved gain allows generation of pulses with energy of ~ 480 nJ.

After amplification, the pulse duration turns out to be somewhat shorter than before: the oscillograms in Fig. 12 demonstrate that 1-ns laser pulses shorten to 0.9-ns pulses upon amplification. The cause of this shortening may be attributed both to dispersive compression coming from the anomalous dispersion of the active fiber and to the spectral

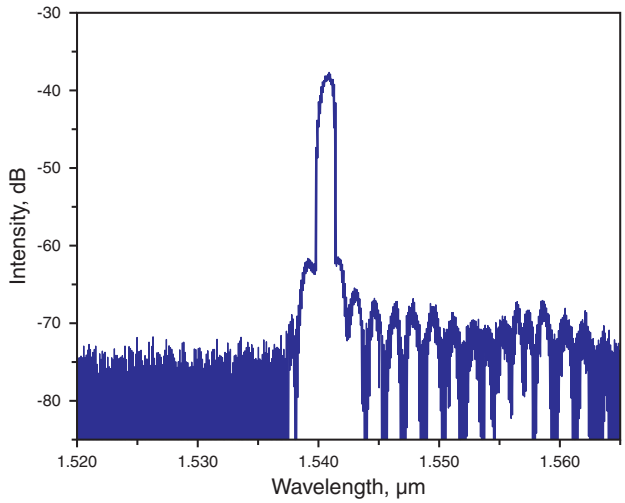

Figure 11 (online color at www.lphys.org) Optical spectrum of the laser radiation upon amplification in the double-pass EDFA with an FBG

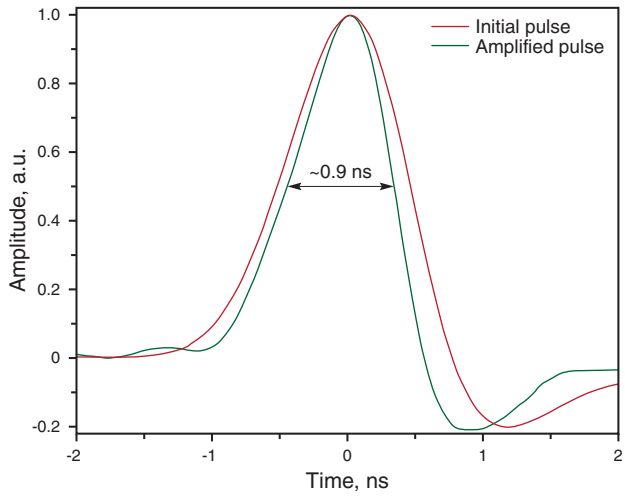

Figure 12 (online color at www.lphys.org) Oscillograms of laser pulses before (red) and after (dark green) amplification

filtering by optical elements with limited bandwidth that clips the wings of strongly chirped laser pulses.

It is important to note that a rough estimate of the time-bandwidth product of pulses emitted by the laser yields a figure of more than 100 that may evidence giant chirp in the laser pulses. The net normal dispersion of the laser cavity ensures the positive sign of the chirp.

Taking into account the fact that the dispersion of the active fiber used in the EDFA ($\sim$ 16 ps/nm/km @ 1540 nm) is comparable to that of conventional telecommunication fibers which comply with G.652 standard, we also investigated the possibility and efficiency of in-fiber

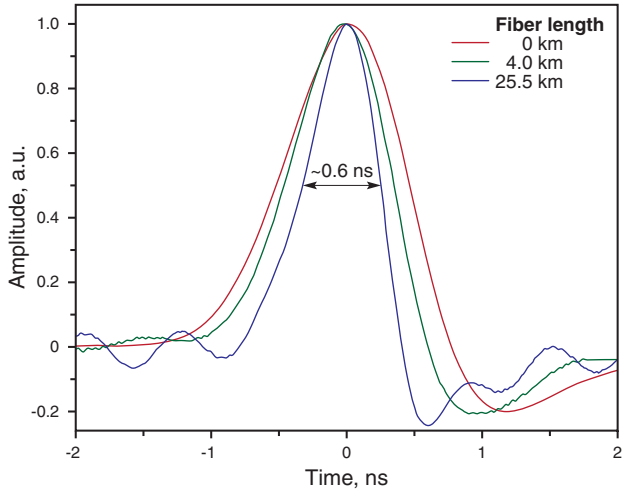

Figure 13 (online color at www.lphys.org) Oscillograms of laser pulses before (red) and after (green and blue) propagation over different lengths of the anomalous-dispersion passive fiber

dispersive compression of the laser pulses by using such a telecom fiber.

We have examined the compression of pulses using a single-mode fiber Sumitomo Pure Access. This fiber has anomalous chromatic dispersion of about 17 ps/nm/km (the slope of the dispersion curve is $\sim$ 0.09 ps/nm^2/km) at the laser wavelength. The following results were obtained: substantial shortening of the laser pulses only occurs upon propagation through very long (kilometer-scale) sections of the fiber. Even for a moderate compression comparable to the pulse shortening in the amplifier, a 1-ns pulse emitted by the laser has to travel about 4 km along the above-named passive single-mode fiber with anomalous dispersion. Oscillograms in Fig. 13 illustrate the pulse compression effects resulted from propagation over the different lengths of the Sumitomo Pure Access fiber. The pulses were finally compressed down to 0.6 ns in a 25.5-km-long section of this fiber.

Insignificant pulse shortening that we observed in the anomalous-dispersion passive fiber cannot be fully attributed to conventional linear dispersive compression. One of the possible reasons for low compressibility may be a complex structure of the laser pulses [22] or significant nonlinearity of their chirp. Nevertheless the obtained experimental results promise the possibility of more substantial compression of such pulses in sufficiently long single-mode telecommunication fibers of standard G.652. The price of such compression would be a loss of the radiation energy due to optical fiber losses.

4. Conclusion

We have proposed a new design of fiber laser cavity – "γ-configuration", that offers a range of new functionalities

for management and optimization of mode-locked lasing regimes. This novel cavity configuration has been successfully implemented into a long-cavity normal-dispersion self-mode-locked Er-fiber laser. The conducted experimental study has shown that the new cavity design allows for efficient compensation or elimination of most destructive factors that affect lasing dynamics and output parameters of such lasers. In particular, it features compensation for polarization instability, suppression of ASE, reduction of pulse duration, prevention of in-cavity wave breaking, and stabilization of the lasing wavelength. This laser along with a specially designed double-pass EDFA have allowed us to demonstrate an environmentally stable all-fiber laser system able to deliver sub-nanosecond high-energy pulses with low level of ASE noise. The combination of high pulse energy and short pulse duration extends the range of practical applications of long-cavity mode-locked fiber lasers with normal dispersion.

Acknowledgements This work was partially supported by the Council of the President of the Russian Federation for the Leading Research Groups of Russia (project No. NSh-4339.2010.2), by the Russian Foundation for Basic Research (projects No. 10-02-91157-GFEN_a and No. 10-02-00987_a), and by the Leverhulme Trust and the Marie Curie FP7 Program IRSES.

References

[1] S. Kobtsev, S. Kukarin, and Y. Fedotov, Opt. Express **16**, 21936–21941 (2008).
[2] B. Ibarra-Escamilla, O. Pottiez, E.A. Kuzin, R. Grajales-Coutiño, and J.W. Haus, Laser Phys. **18**, 914–919 (2008).
[3] X.L. Tian, M. Tang, P.P. Shum, Y.D. Gong, C.L. Lin, S.N. Fu, and T.S. Zhang, Opt. Lett. **34**, 1432–1434 (2009).
[4] X.L. Tian, M. Tang, X.P. Cheng, P.P. Shum, Y.D. Gong, and C.L. Lin, Opt. Express **17**, 7222–7227 (2009).
[5] M. Zhang, L.L. Chen, C. Zhou, Y. Cai, L. Ren, and Z.G. Zhang, Laser Phys. Lett. **6**, 657–660 (2009).
[6] E.J.R. Kelleher, J.C. Travers, E.P. Ippen, Z. Sun, A.C. Ferrari, S.V. Popov, and J.R. Taylor, Opt. Lett. **34**, 3526–3528 (2009).
[7] L. Chen, M. Zhang, C. Zhou, Y. Cai, L. Ren, and Z. Zhang, Electron. Lett. **45**, 731–733 (2009).
[8] S.M. Kobtsev, S.V. Kukarin, S.V. Smirnov, and Y.S. Fedotov, Laser Phys. **20**, 351–356 (2010).
[9] V.I. Denisov, B.N. Nyushkov, and V.S. Pivtsov, Proc. SPIE **7580**, 75802U (2010).
[10] V.I. Denisov, B.N. Nyushkov, and V.S. Pivtsov, Quantum Electron. **40**, 25–27 (2010).
[11] B.N. Nyushkov, V.I. Denisov, S.M. Kobtsev, V.S. Pivtsov, N.A. Kolyada, A.V. Ivanenko, and S.K. Turitsyn, Laser Phys. Lett. **7**, 661–665 (2010).
[12] Y. Senoo, N. Nishizawa, Y. Sakakibara, K. Sumimura, E. Itoga, H. Kataura, and K. Itoh, Opt. Express **18**, 20673–20680 (2010).
[13] L.J. Kong, X.S. Xiao, and C.X. Yang, Laser Phys. Lett. **7**, 359–362 (2010).
[14] X.H. Li, X.M. Liu, X.H. Hu, L.R. Wang, H. Lu, Y.S. Wang, and W. Zhao, Opt. Lett. **35**, 3249–3251 (2010).
[15] D. Mao, X.M. Liu, L.R. Wang, H. Lu, and H. Feng, Opt. Express **18**, 23024–23029 (2010).
[16] J.-H. Lin, D. Wang, and K.-H. Lin, Laser Phys. Lett. **8**, 66–70 (2011).
[17] R. Song, H.-W. Chen, S.-P. Chen, J. Hou, and Q.-S. Lu, J. Opt. **13**, 035201 (2011).
[18] F. Ai, Z.G. Cao, X.F. Zhang, C.M. Zhang, B. Zhang, and B.L. Yu, Opt. Laser Technol. **43**, 501–505 (2011).
[19] J.C. Travers, J. Morgenweg, E.D. Obraztsova, A.I. Chernov, E.J.R. Kelleher, and S.V. Popov, Laser Phys. Lett. **8**, 144–149 (2011).
[20] N. Akhmediev and A. Ankiewicz (eds.), Dissipative Solitons, Lecture Notes in Physics, Springer Series, vol. 661 (Springer, Berlin-Heidelberg, 2005).
[21] W.H. Renninger, A. Chong, and F.W. Wise, Phys. Rev. A **77**, 023814 (2008).
[22] G.P. Agrawal, Nonlinear Fiber Optics, 2nd ed. (Academic Press, New York, 1995).
[23] L.J. Kong, X.S. Xiao, and C.X. Yang, Laser Phys. **20**, 834–837 (2010).
[24] D. Mao, X.M. Liu, L.R. Wang, X.H. Hu, and H. Lu, Laser Phys. Lett. **8**, 134–138 (2011).
[25] S. Kobtsev, S. Kukarin, S. Smirnov, S. Turitsyn, and A. Latkin, Opt. Express **17**, 20707–20713 (2009).
[26] B.N. Nyushkov, I.I. Korel, V.I. Denisov, V.S. Pivtsov, and N.A. Kolyada, Proc. SPIE **7994**, 799406 (2010).
[27] L.E. Nelson, D.J. Jones, K. Tamura, H.A. Haus, and E.P. Ippen, Appl. Phys. B **65**, 277–294 (1997).
[28] F.W. Wise, A. Chong, and W.H. Renninger, Laser Photon. Rev. **2**, 58–73 (2008).
[29] S.M. Kobtsev, S.V. Kukarin, and S.V. Smirnov, Laser Phys. **20**, 375–378 (2010).
[30] D.M. Brown, K.B. Shi, Z.W. Liu, and C.R. Philbrick, Opt. Express **16**, 8457–8471 (2008).
[31] T. Erdogan, J. Lightwave Technol. **15**, 1277–1294 (1997).
[32] C.B. Mou, K.M. Zhou, L. Zhang, and I. Bennion, J. Opt. Soc. Am. B **26**, 1905–1911 (2009).
[33] C.B. Mou, H. Wang, B.G. Bale, K.M. Zhou, L. Zhang, and I. Bennion, Opt. Express **18**, 18906–18911 (2010).
[34] H. Inaba, Y. Akimoto, K. Tamura, E. Yoshida, T. Komukai, and M. Nakazawa, Opt. Commun. **180**, 121–125 (2000).
[35] A.-P. Luo, Z.-C. Luo, W.-C. Xu, V.V. Dvoyrin, V.M. Mashinsky, and E.M. Dianov, Laser Phys. Lett. **8**, 601–605 (2011).
[36] X.H. Li, Y.S. Wang, W. Zhao, W. Zhang, Z. Yang, X.H. Hu, H.S. Wang, X.L. Wang, Y.N. Zhang, Y.K. Gong, C. Li, and D.Y. Shen, Laser Phys. **21**, 940–944 (2011).
[37] B.G. Bale and S. Wabnitz, Opt. Lett. **35**, 2466–2468 (2010).
[38] B.G. Bale, J.N. Kutz, A. Chong, W.H. Renninger, and F.W. Wise, J. Opt. Soc. Am. B **25**, 1763–1770 (2008).
[39] B.G. Bale and J.N. Kutz, in: Proc. of the World Congress on Engineering, London, UK, July 1–3, 2009 (WCE 2009), vol. 1, pp. 367–370.
[40] L.M. Zhao, D.Y. Tang, J. Wu, X.Q. Fu, and S.C. Wen, Opt. Express **15**, 2145–2150 (2007).
[41] A.I. Chernykh and S.K. Turitsyn, Opt. Lett. **20**, 398–400 (1995).
[42] L. Kramer, E.A. Kuznetsov, S. Popp, and S.K. Turitsyn, JETP Lett. **61**, 904–910 (1995).